ChemComm

Accepted Manuscript

This article can be cited before page numbers have been issued, to do this please use: C. Zhu, M. Liu, X. Li , X. Zhang and J. Chen, *Chem. Commun.*, 2018, DOI: 10.1039/C8CC05829F.

This is an Accepted Manuscript, which has been through the Royal Society of Chemistry peer review process and has been accepted for publication.

Accepted Manuscripts are published online shortly after acceptance, before technical editing, formatting and proof reading. Using this free service, authors can make their results available to the community, in citable form, before we publish the edited article. We will replace this Accepted Manuscript with the edited and formatted Advance Article as soon as it is available.

You can find more information about Accepted Manuscripts in the author guidelines.

Please note that technical editing may introduce minor changes to the text and/or graphics, which may alter content. The journal's standard Terms & Conditions and the ethical guidelines, outlined in our author and reviewer resource centre, still apply. In no event shall the Royal Society of Chemistry be held responsible for any errors or omissions in this Accepted Manuscript or any consequences arising from the use of any information it contains.

ROYAL SOCIETY OF CHEMISTRY

rsc.li/chemcomm

View Article Online
DOI: 10.1039/C8CC05829F

Journal Name

COMMUNICATION

A new electrochemical aptasensor for sensitive assay of protein based on dual-signaling electrochemical ratiometric method and DNA walker strategy

Received 00th January 20xx,
Accepted 00th January 20xx

DOI: 10.1039/x0xx00000x

www.rsc.org/

Caixia Zhu, Mengyue Liu, Xiaoyu Li, Xiaohua Zhang and Jinhua Chen*

Herein, a new electrochemical aptamer-based biosensor for highly sensitive assay of thrombin has been developed based on the dual-signaling electrochemical ratiometric method and the DNA walker strategy, and shows a low detection limit of about 56 fM.

As is well-known, electrochemical aptamer-based biosensors have received much attention because of their advantages of simplicity, high sensitivity, good selectivity and low cost for target assay.[1] They have been widely applied in the detection of various analytes, such as cocaine,[2] lysozyme,[3] thrombin,[4] adenosine triphosphate,[2c,5] and platelet-derived growth factor.[6] In order to enhance the sensitivity of the electrochemical aptamer-based biosensors, many signal amplification strategies, including nanomaterials-based strategies[7] (such as gold nanoparticles,[8] graphene,[9] quantum dots,[10] etc.) and DNA-based methods (such as strand displacement amplification,[11] rolling circle amplification,[12] polymerase chain reaction, [13] etc.), have been developed. Recently, an interesting signal amplification strategy based on DNA-based machines (typically, DNA walkers) has been received more and more attention.[14] DNA walkers are a type of molecular machine based on a burnt-bridge mechanism in which sequential oligonucleotide hybridization is followed by toehold-mediated strand displacement.[15] Yang et al. reported a DNA nanomachine based on a DNA-functionalized gold nanoparticle (DNA-AuNP) for DNA assay.[16] Qu et al. developed an exonuclease III (Exo III)-powered stochastic DNA walker and explored its application in highly sensitive detection of bacteria.[17] Ji et al. proposed a binding-induced DNA walker aptasensor for TB assays.[18] However, most of these DNA-based machines have only one response signal, either the type of "signal-on" or "signal-off". To avoid the limitation of the "signal-off" strategy and to make use of the superiority of the "signal-on" strategy, the ratiometric electrochemical assay, combining "signal-on" and "signal-off" probes, has been developed recently due to its good analytical performances (such as low detection limit, wide linear range, good reliability and reproducibility, and low background noise) [19] and simple equipments originated from electrochemical methods (superior to other methods, such as surface-enhanced Raman scattering),[20] which inspired researchers to construct electrochemical aptamer-based biosensors by combining the advantages of the dual-signaling electrochemical ratiometric method and the DNA walker strategy. However, till now, only one work focused on this topic based on DOX encapsulated mesoporous Pt nanospheres as a "signal-on" probe and MB-labeled DNA as a "signal-off" probe [21], which suffered from that the synthesis of such nanospheres was time-consuming, complex and not easy to control. The new ratiometric electrochemical aptamer-based biosensor with DNA walker strategy is still desirable.

Herein, taking thrombin (TB) as a model due to its crucial role in cardiovascular diseases, regulation of inflammation processes and anti-clotting therapeutics,[22] a new electrochemical aptamer-based biosensor has been developed for sensitive assay of protein based on DNA-based dual-signaling electrochemical ratiometric method and DNA walker strategy. As shown in Scheme 1, a double-stranded DNA was prepared by hybridizing the DNA walkers (DWs) and the thrombin aptamer (TBA), and then the DWs/TBA double-stranded DNA and methylene blue-labeled DNA (MB-DNA) were immobilized on the surface of the gold nanoparticles (Au NPs) modified glassy carbon electrode (GCE). When the ferrocene-labeled (Fc-DNA) was added, the MB-DNA hybridized with the Fc-DNA to form a MB-DNA/Fc-DNA duplex. In the presence of TB, DWs could be released due to the specific interaction between TB and its aptamer (TBA). The released DWs hybridized with part of Fc-DNA in MB-DNA/Fc-DNA duplex and a duplex with a blunt end at the 3'-termini of Fc-DNA was formed, which triggered the Exo III cleavage process accompanied by throwing away of Fc from the electrode and releasing of DWs. And the DWs continued to

State Key Laboratory of Chemo/Biosensing and Chemometrics, College of Chemistry and Chemical Engineering, Hunan University, Changsha, 410082, P.R. China.
E-mail: chenjinhua@hnu.edu.cn; Fax: +86-731-88821848; Tel: +86-731-88821848.
† Electronic Supplementary Information (ESI) available: DNA sequences used in this work; Experimental section; Characterization of the electrode; Polyacrylamide gel electrophoresis; Feasibility of the biosensors; Optimization of experimental conditions; Recovery test. See DOI: 10.1039/x0xx00000x

View Article Online
DOI: 10.1039/C8CC05829F

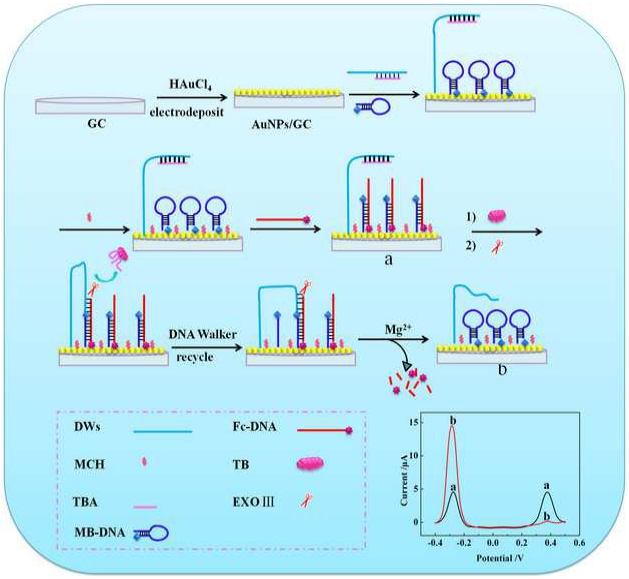

Scheme 1 The schematic illustration of the electrochemical aptamer-based biosensor for TB assay.

hybridize the another Fc-DNA to perform the DNA walker recycling process. The remaining single-stranded MB-DNA could form a hairpin structure in the presence of magnesium ions (Mg^{2+}) due to its tailor-made complementary bases at both ends.[23] This resulted in an enhancement of MB signal (I_{MB}) and a suppression of Fc signal (I_{Fc}). Based on the value of I_{MB}/I_{Fc}, the proposed electrochemical aptamer-based biosensor showed superior analytical performance for sensitive assay of TB with a linear range from 0.1 pM to 10 pM and a low detection limit of 56 fM.

The SEM images of the GCE and Au NPs/GCE are shown in Fig. S1 (ESI†). It can be seen that Au NPs have a uniform distribution on the GCE surface (Fig. S1B) and the particle size of the Au NPs is about 30 - 120nm. It is clear that Au NPs on the GCE provide a large surface area for the immobilization of DWs/TBA double-stranded DNA and MB-DNA, and the electron transfer ability of the GCE should also be improved due to the excellent electrochemical properties of Au NPs.

The step-by-step modification of GCE was characterized by cyclic voltammetry (CV). As shown in Fig. 1A, compared with the bare GCE (curve a, Fig. 1A), the peak currents of the AuNPs/GCE (curve b, Fig. 1A) increase and the corresponding peak potential difference decreases. This implies that the AuNPs/GCE possesses excellent electron transfer properties due to the good electrochemical properties of AuNPs. When the DWs/TBA double-stranded DNA and MB-DNA are immobilized on the AuNPs/GCE, the peak currents decrease obviously (curve c, Fig. 1A). Afterward, when the surface of the electrode is further blocked by 6-mercaptohexanol (MCH), the CV peak currents further decrease and the corresponding peak potential difference increases (curve d, Fig. 1A), indicating that the electron transport of $[Fe(CN)6]^{3-/4-}$ ions at the electrode surface is inhibited due to the nonconductive property of MCH. As expected, the hybridization between Fc-DNA and MB-DNA

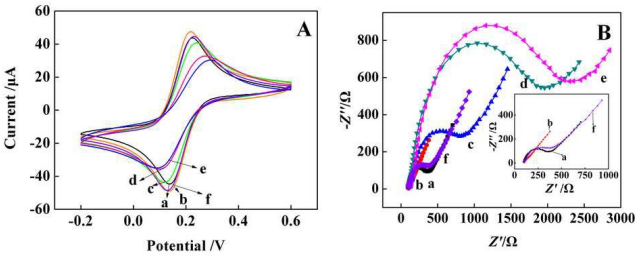

Fig. 1. (A) cyclic voltammograms and (B) EIS results of the different modified GCE in $[Fe(CN)6]^{3-/4-}$ (5 mM) + KCl (0.1 M) aqueous solution. The impedance spectra were recorded in the range of 0.1 Hz-100 kHz with AC amplitude of 5 mV and cyclic voltammetry experiments were performed at a scan rate of 100 mV s^{-1}. (a) bare GCE, (b) AuNPs/GCE, (c) MB-DNA/DWS/TBA/AuNPs/GCE, (d) MCH/MB-DNA/DWS/TBA/AuNPs/GCE, (e) Fc-DNA/MCH/MB-DNA/DWS/TBA/AuNPs/GCE, (f)Fc-DNA/MCH/MB-DNA/DWS/TBA /AuNPs/GCE after incubated with Exo III and TB.

to form a MB-DNA/Fc-DNA duplex decreases further the peak currents (curve e, Fig. 1A). However, after incubated with TB and Exo III, the peak currents (peak potential difference) of the Fc-DNA/MCH/MB-DNA/DWS/TBA/AuNPs/GCE increase (decreases) obviously (curve f, Fig. 1A). This indicates the successful Exo III cleavage and DNA walking processes, which are also confirmed by gel electrophoresis data (Fig. S2, ESI†).

On the other hand, electrochemical impedance spectroscopy (EIS) method was further employed to characterize the stepwise modification of the electrode. In a typical Nyquist plots of EIS results, the semicircle section at high frequency range corresponds to the charge transfer limited process, and the value of the diameter of the semicircle reflects the interfacial charge-transfer resistance (R_{ct}).[24] As shown in Fig. 1B, the bare GCE shows a small semicircle domain (R_{ct} = 333.3 Ω, curve a, Fig. 1B), implying a good electron-transfer process. For the AuNPs modified GCE, the R_{ct} value (curve b, Fig. 1B) decreases to 112.3 Ω, suggesting that the electron transfer ability of the GCE is enhanced due to the excellent electrochemical properties of AuNPs. The successive modification processes on the AuNPs/GCE (immobilizations of DWs/TBA double-stranded DNA and MB-DNA, self-assembly of MCH and the hybridization between Fc-DNA and MB-DNA) lead to the successively increase of the R_{ct} value due to their blocking effect on the electron transfer process of redox probe at the electrode (from curves c to e, Fig. 1B). When the electrode is further incubated with TB and Exo III, the R_{ct} value decreases to 461.7 Ω (curve f, Fig. 1B). These results are in accordance with that observed in CV investigation (Fig. 1A), implying that the electrochemical aptamer-based biosensor has been fabricated successfully according to Scheme 1.

The feasibility of the proposed biosensor for TB assay were evaluated by square wave voltammetry (SWV) and the corresponding results are shown in Fig. S3 (ESI†). In the absence of both TB and Exo III (curve a, Fig. S3), the oxidation peak currents of both MB and Fc are observed. With the addition of Exo III (curve b, Fig. S3), no obvious changes of SWV peak currents are observed. However, in the presence of both TB and Exo III, it can be observed obviously that the

View Article Online
DOI: 10.1039/C8CC05829F

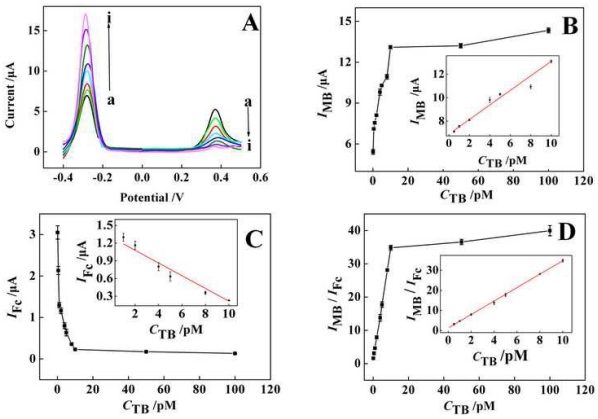

Fig. 2. (A) SWV responses of the developed method to different concentration of TB (from a to h): 0.1 pM, 0.5 pM, 1 pM, 2 pM, 4 pM, 5 pM, 8 pM, 10 pM in 0.1 M PBS (pH 7.0) containing 0.1 M KCl. (B) Dependence of I_{MB} on TB concentration. (C) Dependence of I_{Fc} on TB concentration. (D) Dependence of (I_{MB}/I_{Fc}) on TB concentration.

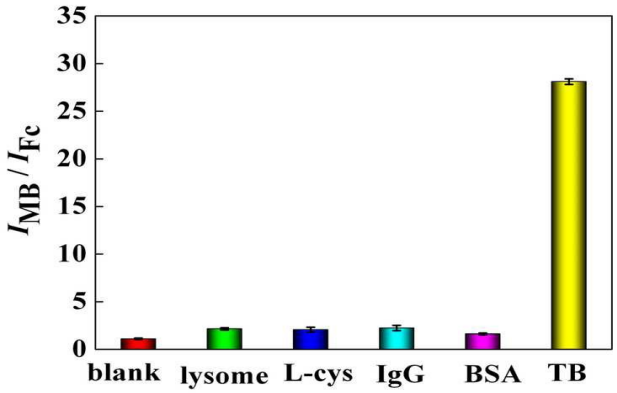

Fig. 3. Selectivity of the developed biosensor to lysome (10nM), L-cys (10nM), IgG (10nM), BSA (10nM) and TB (8 pM).

oxidation peak current of MB increases and that of Fc decreases (curve c, Fig. S3). This clearly indicates that the developed electrochemical aptamer-based biosensor can be adopted for TB detection.

To achieve the optimal analytical results, the experimental conditions, including the number of thymine (T) in DWs, the reaction time between TB and TBA, and the reaction time of Exo III cleavage, were optimized. Fig. S4A (ESI†) indicates that the ratio (I_{MB}/I_{Fc}) between the oxidation peak currents of MB (I_{MB}) and Fc (I_{Fc}) increases with the increase of the number of T in DWs and reaches to a plateau when the number of T is 40. Therefore, 40-nt T is chosen as the space sequence in swing arm for the optimal signal readout. From Fig. S4B (ESI†), it is noted that the I_{MB}/I_{Fc} value increases with the increase of the TB reaction time. After the TB reaction time is more than 60 min, the I_{MB}/I_{Fc} value has almost no increase. Thus, the optimal TB reaction time is 60 min. Similarly, for Exo III cleavage process, the I_{MB}/I_{Fc} value increases with the increase of the Exo III cleavage time and reaches a plateau with a slight increase at about 60 min (Fig. S4C, ESI†). In order to ensure the enough cleavage time of Exo III, 80 min is selected as the optimal reaction time for Exo III in the following experiments.

Under the optimal experimental conditions, the analytical performance of the developed electrochemical aptamer-based biosensor for different concentrations of TB was investigated. From Fig. 2A, it is noted that the oxidation peak current of MB increases and the oxidation peak of Fc decreases with the increase of TB concentration. The calibration plots of the developed electrochemical aptamer-based biosensor using individual MB or Fc signal for TB assay are shown in Figs. 2B and 2C. Both of them exhibit good linear relationship between the oxidation peak current and the concentration of TB in the range of 1 pM to 10 pM with detection limits of 0.67 pM (based on MB signal) and 2.54 pM (based on Fc signal) (3σ). Fig. 2D shows the calibration plot of the electrochemical ratiometric assay of TB using I_{MB}/I_{FC} as signal. The I_{MB}/I_{FC} value linearly depends on the TB concentration in the range of 0.1 pM to 10 pM with a detection limit of 0.056 pM (3σ), and the corresponding linear regression equation is (I_{MB}/I_{Fc}) = $3.34923C_{TB}$ (pM)+1.26552 (R^2 = 0.9998). It is clear that the value of limit of detection (LOD) obtained by using "I_{MB}/I_{Fc}" as the response signal is much lower than that obtained by using I_{MB} or I_{Fc} as the response signal. To our best knowledge, the value of LOD obtained by this method is also much lower than that by most of other electrochemical methods reported previously (Table S2, ESI†).

To investigate the specific response of the proposed electrochemical aptamer-based biosensor to TB, control experiments were performed by replacing TB with some typical interfering substances, including lysozyme, L-cys, IgG and BSA. As illustrated in Figure 3, there are no obvious changes when the biosensor is incubated with these interferents. However, the TB sample gives a significant change of the I_{MB}/I_{Fc} value, implying that the developed electrochemical aptamer-based biosensor has high specificity for TB assay due to the specific inaction between TB and TBA. Besides, five different electrodes were used to detect TB (0.1 pM) and the relative standard deviation is 3.04 %. Furthermore, when the electrochemical aptamer-based biosensor was stored at 4 °C for 15 day, the I_{MB}/I_{Fc} value has no significant change. These results indicate that the proposed electrochemical aptamer-based biosensor exhibits satisfactory reproducibility and stability.

For the evaluation of the practical application of the developed electrochemical aptamer-based biosensor, it is very significant and essential to detect TB in complex systems. Healthy human blood serum samples were employed in this paper as the model of complex systems. TB with different concentrations was added in 20-fold diluted human serum sample solutions diluted with 20 mM PBS. From Table S3 (ESI†), it is noted that the recoveries for the added TB with 0.1 pM, 1 pM, 2 pM are 90%, 96%, 105%, respectively. On the other hand, the I_{MB}/I_{FC} values for TB spiked in normal human serum samples are almost same with that in PBS (Fig. S5, ESI†). The results shown in Fig. S5 and Table S3 reveal that the developed

View Article Online
DOI: 10.1039/C8CC05829F

method has satisfactory recoveries and may have great practical applications in TB assay.

In summary, we develop a novel electrochemical aptamer-based biosensor for sensitive and selective assay of TB. In comparison with traditional electrochemical aptamer-based biosensors, the developed electrochemical aptamer-based biosensor exhibits a lower LOD (56 fM) for TB detection due to the combination of two efficient signal amplification strategies. Importantly, the electrochemical aptamer-based biosensor can be easily modified for the detection of arbitrary targets by simply altering its aptamer sequence. This generality provides a great potential in bioanalysis, biomedical research, and early clinical diagnosis.

This work was financially supported by NSFC (21475035, 21727810), and the Foundation for Innovative Research Groups of NSFC (21521063).

Conflicts of interest

There are no conflicts of interest to declare.

Notes and references

1 (*a*) X. R. Zhang, B. P. Qi, Y. Li, S. S. Zhang, *Biosens. Bioelectron.,* 2009, **25,** 259–262. (*b*) J. C. Yu, L. Q. Zhang, X. Xu, S. Q. Liu, *Anal. Chem.,* 2014, **86,** 10741-10748. (*c*) J. Zhao, M. L. Liu, Y. Y. Zhang, H. T. Li, Y.H. Lin, S. Z. Yao, *Anal. Chim. Acta*., 2013, **759**, 53–60. (*d*) X. X. Li, H. L. Qi, L. H. Shen, Q. Gao, C. H. Zhang, *Electroanalysis* , 2008, **20**, 1475–1482. (*e*) M. Labib, A. S. Zamay, D. Muharemagic, A. V. Chechik, J. C. Bell, M. V. Berezovski, *Anal. Chem.,* 2012, **84**, 1813–1816. (*f*) F. J. Hernandez, V. C. Ozalp, *Biosensors*, 2012, **2,** 1–14.

2 (*a*) Y. Du, C. G. Chen, J. Y. Yin, B. L. Li, M. Zhou, S. J. Dong, E. K. Wang, *Anal. Chem.,*2010, **82**, 1556–1563. (*b*) B. R. Baker, R. Y. Lai, M. S. Wood, E. H. Doctor, A. J. Heeger, K. W. Plaxco, *J. Am. Chem. Soc.,* 2006, **128,** 3138–3139. (*c*) Y. L. Wen, H. Pei, Y. Wan, Y. Su, Q. Huang, S. P. Song, C. H. Fan, *Anal. Chem.,* 2011, **83**, 7418–7423. (*d*) J. S. Swensen, Y. Xiao, B. S. Ferguson, A. A. Lubin, R. Y. Lai, A. J. Heeger, K. W. Plaxco, H. T. Soh, J. *Am. Chem. Soc.,* 2009, **131**, 4262–4266. (*e*) E. Golub, G. Pelossof, R. Freeman, H. Zhang, I. Willner, *Anal. Chem.,* 2009, **81,** 9291–9298.

3 (*a*) L. D. Li, Z. B. Chen, H. T. Zhao, L. Guo, X. J. Mu, *Sens. Actuators, B.*, 2010, **149,** 110–115. (*b*) Z. B. Chen, J. X. Guo, *Electrochim. Acta.,* 2013, **111**, 916–920.

4 (*a*) Y. Xiao, B. D. Piorek, K. W. Plaxco, A. J. Heeger, *J. Am. Chem. Soc.,* 2005, 127, 17990–17991. (*b*) Y. Xiao, A. A. Lubin, A. J. Heeger, K. W. Plaxco, *Angew. Chem. Int. Ed.,* 2005, **44**, 5456–5459. (*c*) Y. Lu, X. C. Li, L. M. Zhang, P. Yu, L. Su, L. Q. Mao, *Anal. Chem.,* 2008*,* **80,** 1883– 1890. (*d*) J. H. Chen, J. Zhang, J. Li, H. H. Yang, F. F. Fu, G. N. Chen, *Biosens. Bioelectron.,* 2010, **25**, 996–1000.

5 (*a*) L. Kashefi-Kheyrabadi, M. A. Mehrgardi, *Biosens. Bioelectron.,* 2012, **37**, 94–98. (*b*) X. L. Zuo, S. P. Song, J. Zhang, D. Pan, L. H. Wang, C. H. Fan, *J. Am. Chem. Soc.,* 2007, **129**, 1042–1043.

6 (*a*) Y. L. Zhang, Y. Huang, J. H. Jiang, G. L. Shen, R. Q. Yu, *J. Am. Chem. Soc.*,2007, **129**, 15448–15449. (*b*) R. Y. Lai, K. W. Plaxco, A. J. Heeger, *Anal. Chem.,* 2007, **79**, 229–233.

7 L. Wu, E. H. Xiong, X. Zhang, X. H. Zhang, J. H. Chen, *Nano Today.,* 2014, **9,** 197-211.

8 S. Pinijsuwan, P. Rijiravanich, M. Somasundrum, W. Surareungchai, *Anal. Chem*., 2008, **80,** 6779−6784.

9 W. Li, P. Wu, H. Zhang, C. X. Cai, *Anal. Chem.,* 2012, **84,**7583–7590.

10 H. Peng, L. J. Zhang, T. H. M. Kjallman, C. Soeller, J. Travas-Sejdic, *J. Am. Chem. Soc.,* 2007, **129,** 3048−3049.

11 (*a*) F. He, F. D. Feng, X. R. Duan, S. Wang, Y. L. Li, D. B. Zhu, *Anal. Chem*., 2008, **80,** 2239−2243. (*b*) C. Wang, H. Zhou, W. P. Zhu, H. B. Zhu, J. H. Jiang, G. L. Shen, R. Q. Yu, *Biosens. Bioelectron*., 2013, **47,** 324−328. (*c*) H. Zhou, S. J. Xie, S. B. Zhang, G. L. Shen, R. Q. Yu, Z. S. Wu, *Chem. Commun.,* 2013, **49,** 2448−2450.

12 (*a*) G. Nallur, C. H. Luo, L. H. Fang, S. Cooley, V. Dave, J. Lambert, K. Kukanskis, S. Kingsmore, R. Lasken, B. Schweitzer, *Nucleic Acids Res*., 2001, **29,** e118. (*b*) J. H. Li, T. Deng, X. Chu, R. H. Yang, J. H. Jiang, G. L. Shen, R. Q. Yu, *Anal. Chem.,* 2010, **82,** 2811−2816. *c*) H. X. Ji, F. Yan, J. P. Lei, H. X. Ju, *Anal. Chem.,* 2012, **84,** 7166−7171. (*d*) W. Zhao, M. M. Ali, M. A Brook, Y. Li, *Angew. Chem., Int. Ed*., 2008, **47,** 6330−6337. (*e*) W. Cheng, W. Zhang, Y. R. Yan, B. Shen, D. Zhu, P. H. Lei, S. J. Ding, *Biosens. Bioelectron.,* 2014, **62,** 274−279. (*f*) P. He, W. P. Qiao, L. J. Liu, S. S. Zhang, *Chem. Commun*., 2014, **50,** 10718−10721. *g*) W. D. Xu, R. J. Deng, L. D. Wang, J. H. Li, *Anal. Chem*., 2014, **86,** 7813−7818.

13 (*a*) R. Y. Lai, E. T. Lagally, S. H. Lee; H. T. Soh, K. W. Plaxco, A. J. Heeger, *Proc. Natl. Acad. Sci. U. S. A.,* 2006, **103,** 4017−4021. (*b*) H. K. Li, J. H. Huang, J. H. Lv, H. J. An, X. D. Zhang, Z. Z. Zhang, C. H. Fan, J. Hu, *Angew. Chem., Int. Ed.,* 2005, **44,** 5100−5103. (*c*) R. K. Saiki, S. Scharf, F. Faloona, K. B. Mullis, G. T. Horn, H. A. Erlich, N. Arnheim, *Science,* 1985, **230,** 1350−1354.

14 (*a*) H. Peng, X. F. Li, H. Zhang, X. C. Le, *Nat. Commun.,* 2017, **8**, 14378. (*b*) C. Jung, P. B. Allen, A. D. Ellington, *Nat. Nanotechnol.,* 2016, **11**, 157-163. (*c*) Z. Q. Xu, L. L. Liao, Y. Q. Chai, H. J. Wang, R. Yuan, *Anal. Chem.,* 2017, **89,** 8282-8287. (*d*) S. Z. Lv, K. Y. Zhang, Y. Y. Zeng, D. P. Tang, *Anal. Chem.,* 2018, **90,** 7086−7093.

15 (*a*) T. Omabegho, R. Sha, N. C. Seeman, *Science*, 2009, **324,** 67 –71; (*b*) S. F. J. Wickham, M. Endo, Y. Katsuda, K. Hidaka, J. Bath,H. Sugiyama, A. J. Turberfield, *Nat. Nanotechnol.,* 2011, **6,** 166 –169; (*c*) S. F. J. Wickham, J. Bath, Y. Katsuda, M. Endo, K.Hidaka, H. Sugiyama, A. J. Turberfield, *Nat. Nanotechnol.,* 2012, **7**, 169 – 173.

16 X. L. Yang, Y. N. Tang, S. D. Mason, J. B. Chen, F. Li, *ACS Nano.,* 2016, **10,** 2324.

17 X. M. Qu, D. Zhu, G. B. Yao, S. Su, J. Chao, H. J. Liu, X. L. Zuo, L. H. Wang, J. Y. Shi, L. H. Wang, W. Huang, H. Pei and C. H. Fan, *Angew. Chem. Int. Ed.*, 2017, **56,** 1855-1858.

18 Y. H. Ji, L. Zhang, L. Y. Zhu, J. P. Lei, J. Wu, H. X. Ju, *Biosens. Bioelectron.,* 2017, **96,** 201–205.

19 (*a*) P. Yu, J. W. Zhou, L. Wu, E. H. Xiong, X. H. Zhang, J. H. Chen, *J. Electroanal. Chem.,* 2014, **732,** 61-65. (*b*) Y. Du, B. J. Lim, B. L. Li, Y. S. Jiang, J. L. Sessler, A. D. Ellington, *Anal. Chem.,* 2014, **86,** 8010-8016. (*c*) K. W. Ren, J. Wu, F. Yan, H. X. Ju, *Sci. Rep.,* 2014, **4,** 4360. (*d*)K. W. Ren, J. Wu, F. Yan, Y. Zhang, H. X. Ju, *Biosens. Bioelectron.,* 2015, **66,** 345-349. (*e*) E. H. Xiong, L. Wu, J. W. Zhou, P. Yu, X. H. Zhang, J. H. Chen, *Anal. Chim. Acta.,* 2015, **853,** 242-248.

20 (*a*) Y. D. Sun, P. Peng, R. Y. Guo, H. H. Wang, T. Li, *Biosens. Bioelectron.,* 2018. **104**, 32–38. (*b*) F. F. Yu, M. K. Su, L. Tian, H. Y. Wang, L. L. Liu *Anal. Chem.*, 2018, **90,** 5232-5238.

21 Q. L. Pu, J. L. Li, J. H. Qiu, X. H. Yang, Y. Li, D. Yin, X. Y. Zhang, Y. Y. Tao, S. C. Sheng, G. M. Xie, *Biosens. Bioelectron.,* 2017, **94,** 719–727.

22 S. Centi, S. Tombelli, M. Minunni, M. Mascini, *Anal. Chem.,* 2007, **79,** 1466–1473.

23 (*a*) V. V. Dao, R. H. Guenther, P. F. Agris, *Biochem.*, 1992, **31,** 11012−11019. (*b*)N. B. Ramsing, K. Rippe, T. M. Jovin, *Biochem.,* 1989, **28,** 9528−9535.

24 Y. Cao, S. Zhu, J. C. Yu, X. J. Zhu, Y. M. Yin, G. X. Li, *Anal. Chem.,* 2012, **84,** 4314-4320.